Article

Not peer-reviewed version

Inhibitory Efficacy of Main Components of *Scutellaria baicalensis* on the Interaction between Spike Protein of SARS-CoV-2 and Human Angiotensin Converting Enzyme II

Cheng-Han Lin , Ho-Ju Chang , Meng-Wei Lin , Xin-Rui Yang , Che-Hsiung Lee , Chih-Sheng Lin *

Posted Date: 31 January 2024

doi: 10.20944/preprints202401.2061.v1

Keywords: SARS-CoV-2; Angiotensin-converting enzyme 2 (ACE2); Spike protein; Traditional Chinese medicine; *Scutellaria baicalensis*; Baicalein; Baicalin

Article

Inhibitory Efficacy of Main Components of *Scutellaria baicalensis* on the Interaction between Spike Protein of SARS-CoV-2 and Human Angiotensin Converting Enzyme II

Cheng-Han Lin [1], Ho-Ju Chang [1], Meng-Wei Lin [1], Xin-Rui Yang [1], Che-Hsiung Lee [1,2] and Chih-Sheng Lin [1,3,*]

[1] Department of Biological Science and Technology, National Yang Ming Chiao Tung University, Hsinchu 30068, Taiwan; a0975273923@gmail.com (C.-H.L.); imhrchang@gmail.com (H.-J.C); lmw1018@nycu.edu.tw (M.-W.L.); yllas0315@gmail.com (X.-R.Y.); ikemanleee@gmail.com (C.-H.L); lincs@nycu.edu.tw (C.-S.L.)

[2] Department of Plastic and Reconstructive Surgery, Chang Gung Memorial Hospital, Linkou, Taoyuan country, Taiwan; ikemanleee@gmail.com (C.-H.L)

[3] Center for Intelligent Drug Systems and Smart Bio-devices (IDS²B), National Yang Ming Chiao Tung University, Hsinchu 30068, Taiwan

* Correspondence: lincs@nycu.edu.tw (C.-S.L.); lincs@nycu.edu.tw

Abstract: Blocking the interaction of the SARS-CoV-2 spike protein with the human angiotensin-converting enzyme II (hACE2) protein serves as a therapeutic strategy for treating COVID-19. Traditional Chinese medicine (TCM) treatments containing bioactive products could alleviate the symptoms of severe COVID-19. However, the emergence of SARS-CoV-2 variants has complicated the process of developing broad-spectrum drugs. As such, the aim in this study was to explore the efficacy of TCM treatments for SARS-CoV-2 variants through targeting the interaction of the viral spike protein with the hACE2 receptor. The antiviral activity was systematically evaluated using a pseudovirus system. *Scutellaria baicalensis* was found to be effective against SARS-CoV-2 infection through affecting the interaction of viral spike protein with the hACE2 protein. The active molecules of *S. baicalensis* were identified and analyzed. Baicalein and baicalin, a flavone and a flavone glycoside, respectively, found in *S. baicalensis*, exhibited strong inhibitory activities, targeting the viral spike protein or hACE2 protein, respectively. Under optimized conditions, virus infection was inhibited by 98% via baicalein-treated pseudovirus and baicalin-treated hACE2. In summary, we identified the potential SARS-CoV-2 inhibitors of the interaction of the Omicron spike protein and hACE2 receptor from *S. baicalensis*. Future studies on the therapeutic application of baicalein and baicalin against SARS-CoV-2 variants are needed.

Keywords: SARS-CoV-2; Angiotensin-converting enzyme 2 (ACE2); Spike protein; Traditional Chinese medicine; *Scutellaria baicalensis*; Baicalein; Baicalin

1. Introduction

The coronavirus disease 2019 (COVID-19) pandemic was caused by severe acute respiratory syndrome coronavirus 2 (SARS-CoV-2) and posed threats and challenges to public healthcare systems [1-3]. As the pandemic progressed, SARS-CoV-2 mutated into highly infective strains such as B.1.617.2 (Delta) and BA.2 (Omicron). The emergence of these variants complicated the prevention of infection and the development of broad-spectrum vaccines or drugs [4]. Therefore, compounds with broad-spectrum antiviral activity against SARS-CoV-2 must be found.

SARS-CoV-2 is a positive-sense single-stranded enveloped RNA virus. SARS-CoV-2 contains four major structural proteins that include spike (S), envelope (E), membrane (M), and nucleocapsid genes (N) [5-7]. The rod-shaped protrusion and trimeric spike protein decorate the surface of SARS-CoV-2. The SARS-CoV-2 spike protein binds to the host cell receptor, human angiotensin-converting

 doi:10.20944/preprints202401.2061.v1

enzyme 2 (hACE2), facilitating conformation change and virus entry [8-11]. As a result, blocking the interaction of viral spike protein to hACE2 is a potential therapeutic strategy against COVID-19.

Traditional Chinese medicine (TCM) represents a system of thousands of years of treatment protocols for health, healing, longevity, and complex healthcare [12, 13]. TCM has also contributed to COVID-19 treatment [14, 15]. Taiwan Chingguan-Yihau (NRICM101), a TCM formula targeting viral respiratory infection and immunomodulation reported by the National Research Institute of Chinese Medicine, Taiwan (NRICM), has been commonly recommended and clinically proven to be effective for the treatment of COVID-19 [16-18]. Based on the theoretical TCM system, *Scutellaria baicalensis*, *Houttuynia cordat*, and *Isatis indigotica* in NRICM101 function to clear heat, dry dampness, promote diuresis, detoxify, and reduce swelling [19-21]. In addition to their traditional uses, *S. baicalensis*, *H. cordata*, and *I. indigotica* have been extensively studied for their pharmacological effects against COVID-19 [22-25]; the findings provided promising avenues for the development of antiviral therapies.

This study aimed to discover the active compounds from TCM that disrupt the interaction between the SARS-CoV-2 spike protein and hACE2 to inhibit infection. The inhibitory activities were evaluated against SARS-CoV-2 pseudovirus infection. We investigated the inhibitory efficacy of the main components of *S. baicalensis* on the interaction between the spike protein of SARS-CoV-2 and hACE2.

2. Results

2.1. Establishment of pseudovirus system for evaluating binding efficacy of viral spike protein and hACE2 receptor

A pseudovirus system was established to evaluate the binding efficacy of viral spike protein to the hACE2 receptor. In the pseudovirus system, HEK293T cells stably expressing hACE2, named HEK293T-hACE2, were infected with SARS-CoV-2 spike pseudovirus. The binding efficacy was quantified using the green fluorescent protein (GFP) intensity of the pseudovirus-infected cells. To characterize the hACE2 in the cells, the protein expression and enzyme activity of hACE2 were measured through Western blot and enzyme activity assays, respectively. The protein expression of ACE2 in HEK293T-hACE2 cells was significantly higher than that in HEK293T cells (**Figure 1a**). The results in **Figure 1b** and **1c** show that the hACE2 activity level was higher (6,000 RFU) in HEK293T-hACE2 cells than in HEK293T cells (44 RFU). The above results indicated the overexpression of hACE2 in HEK293T-hACE2 cells compared with that in HEK293T cells ($p < 0.001$).

The SARS-CoV-2 spike pseudovirus was produced with the spike protein on its surface. To verify the incorporation of the spike protein, the surface protein of the pseudovirus was analyzed via Western blotting. The results in **Figure 1d** show specific bands were found in the lanes of the SARS-CoV-2 spike pseudovirus, but no specific band was found in the VSV pseudovirus in the corresponding position. Then, the HEK293T and HEK293T-hACE2 cells were infected with SARS-CoV-2 spike pseudovirus to examine the efficacy with which the cellular hACE2 bound to the viral spike protein. A significant difference was observed between HEK293T and HEK293T-hACE2 cells ($p < 0.001$) (**Figure 1e**). The GFP intensity in HEK293T-hACE2 cells was 6×10^4 RFU, in comparison with the 5×10^3 RFU in HEK293T cells (**Figure 1f**). Overall, the results demonstrated in Figure 1 confirm that hACE2 was overexpressed in HEK293T-hACE2 cells. Additionally, the established SARS-CoV-2 spike pseudovirus efficiently infected HEK293T-hACE2 cells through the interaction between the viral spike protein and hACE2 receptor.

 doi:10.20944/preprints202401.2061.v1

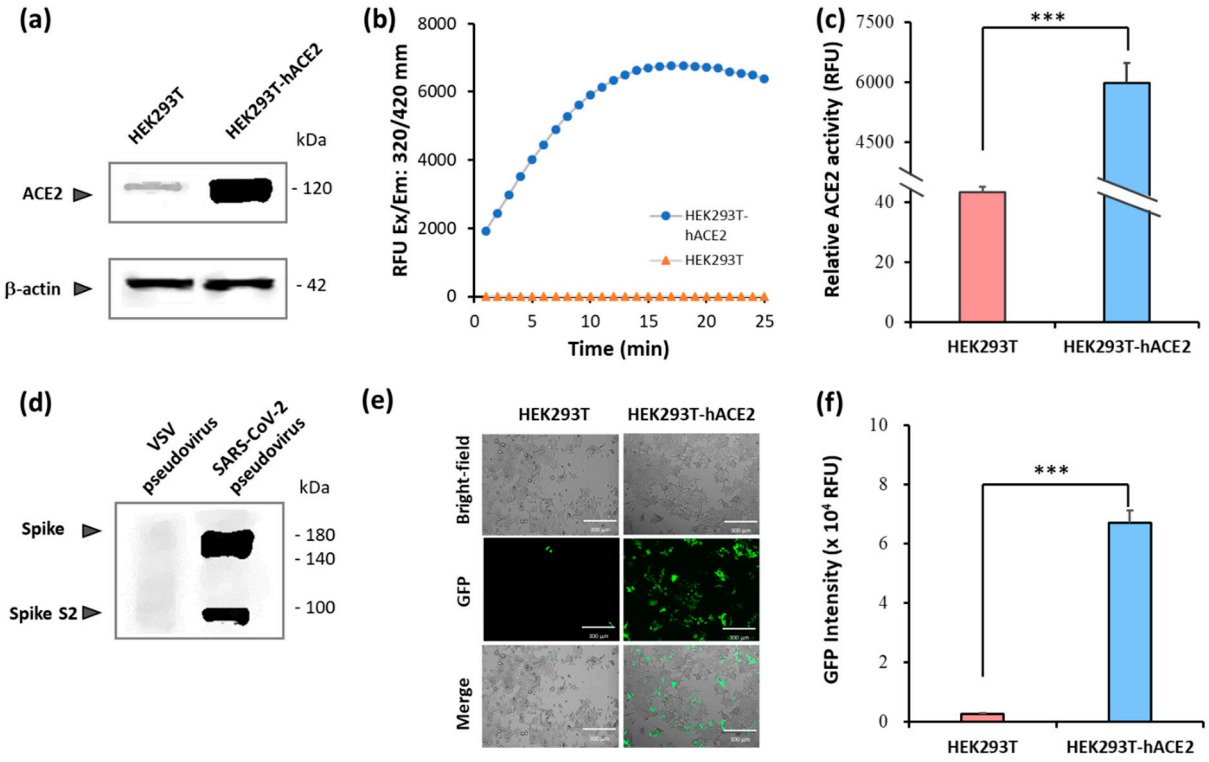

Figure 1. Establishment of SARS-CoV-2 spike pseudovirus system. Protein expression of hACE2 in HEK293T-hACE2 and HEK293T cells was examined via Western blotting analysis (**a**). ACE2 activity in HEK293T-hACE2 and HEK293T cells were examined using ACE2 activity assay (**b**). GFP intensity in HEK293T-hACE2 and HEK293T cells was quantified using a Synergy HT multimode microplate reader (**c**). The spike protein expression of SARS-CoV-2 spike pseudovirus and VSV pseudovirus was examined via Western blotting (**d**). GFP images represent HEK293T-hACE2 and HEK293T cells infected with SARS-CoV-2 spike pseudovirus (**e**). GFP intensity in HEK293T-hACE2 and HEK293T cells was quantified (**f**). All values are expressed as the mean ± SD (n = 5) for each group. The statistical comparison between groups was conducted using Student's t-test; *** $p < 0.001$ vs. HEK293T cells. .

2.2. Identification of SARS-CoV-2 spike pseudovirus system for drug candidates

RNA recombination occurs at a high rate in coronaviruses, increasing plasticity for mutation. SARS-CoV-2 variants were found to increase transmissibility and strengthen the ability to escape immunity. To treat infections with current and future SARS-CoV-2 variants, an Omicron BA.2 spike-protein-expressing pseudovirus was established for the identification of SARS-CoV-2 antiviral drug candidates. As shown in **Figure 2a**, the infection efficiency of the Omicron BA.2 pseudovirus was higher than that of the Wuhan strain. The GFP intensity was as high as 1.3 x 10^5 RFU. The infection efficiency was significantly different between the Omicron BA.2 and Wuhan strains ($p < 0.001$) (**Figure 2b**).

Blocking the interaction between the viral spike protein and cellular hACE2 can be used as a therapy to treat COVID-19. The reproducibility of the pseudovirus system was examined using two typical blockers, a viral spike blocker (cysteamine) [26-27] and a hACE2 blocker (Dalbavancin) [28-29] (**Table 1**). HEK293T-hACE2 cells were pretreated with a putative viral spike blocker and a putative hACE2 blocker for 4 h, and then the cells were infected with pseudovirus (Groups SPC and APC, respectively). BA.2 pseudovirus was pretreated with a spike blocker and a hACE2 blocker for 4 h and then used to infect HEK293T-hACE2 cells (Groups SPV and APV, respectively). Inhibitory activities of viral spike blocker and hACE2 blocker were shown in **Figure 2c**. The inhibitory values of Groups SPC, SPV, APC, and APV were 27.9, 74.2, 76.8, and 51.8%, respectively. The results (**Figure 2d**) showed that the spike and hACE2 blockers inhibited the pseudovirus entry into the cells.

 doi:10.20944/preprints202401.2061.v1

Collectively, these data indicated that the pseudovirus system was successfully established for the evaluation of candidate drugs and therapeutics targeting the virus or cells.

Table 1. Groups in pseudovirus system with putative viral spike protein blocker and putative hACE2 blocker treatments.

Groups	Treatment
SPV	Spike blocker (Cysteamine) pre-treating with SARS-CoV-2 spike pseudovirus
SPC	Spike blocker pre-treating with HEK293T-hACE2 cells
APV	hACE2 blocker (Dalbavancin) pre-treating with SARS-CoV-2 spike pseudovirus
APC	hACE2 blocker pre-treating with HEK293T-hACE2 cells

HEK293T-hACE2 cells were infected with SARS-CoV-2 spike pseudovirus. A putative viral spike protein blocker (cysteamine) and a putative hACE2 blocker (dalbavancin) pre-treated with SARS-CoV-2 spike pseudovirus and HEK293T-hACE2 cells, respectively.

 doi:10.20944/preprints202401.2061.v1

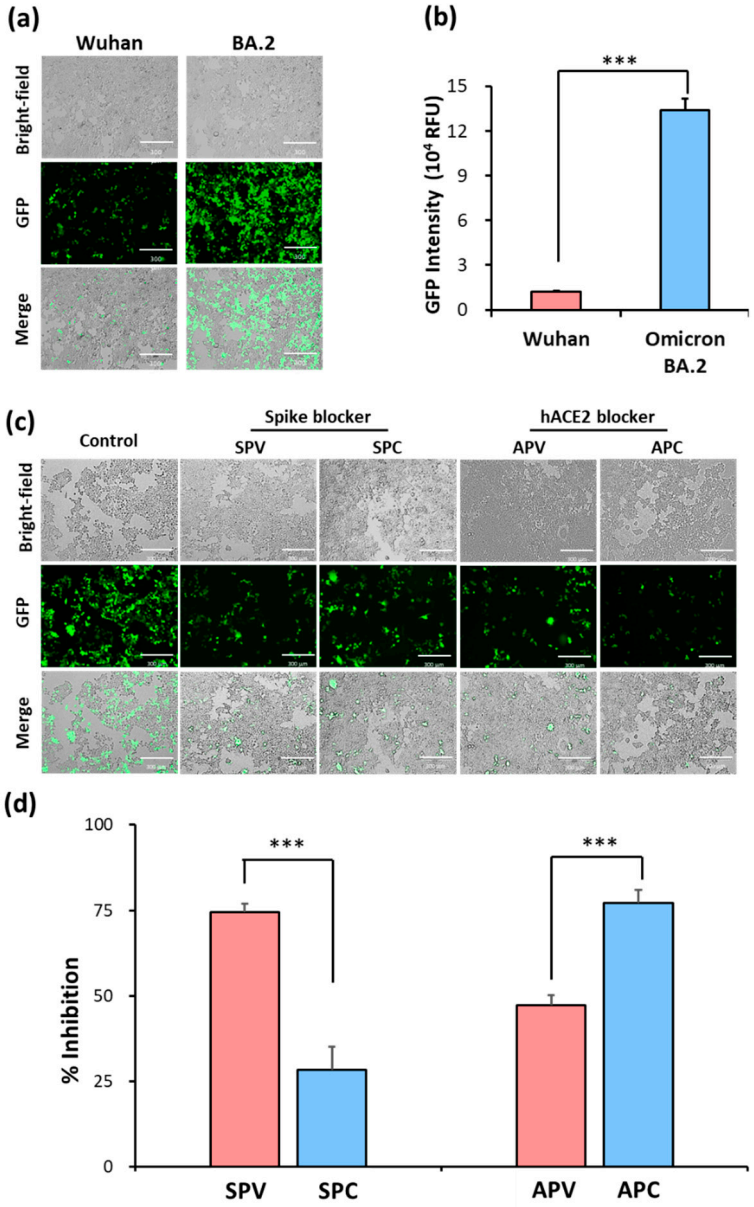

Figure 2. Infection efficiency of SARS-CoV-2 spike variant pseudovirus, and inhibitory efficacy of spike and hACE2 blockers. GFP images represent HEK293T-hACE2 cells that were infected with pseudovirus expressing spike protein of Wuhan or BA.2. strains (**a**). GFP intensity was detected with a Synergy HT multimode microplate reader (**b**). GFP images of HEK293T-hACE2 cells infected with SARS-CoV-2 BA.2 spike pseudovirus (**c**). The inhibitory efficacy of spike and hACE2 blockers preincubated with pseudovirus or cells (**d**). All values are expressed as the mean ± SD (n = 5) for each group. The statistical comparison among groups was conducted using Student's t-test; *** $p < 0.001$ vs. SPV or APV group. SPV, SPC, APV, and APC are defined in **Table 1**.

2.3. Assessment of inhibitory efficacy of herbs on pseudovirus infection

We focused on finding the biologically active components in NRICM101. The *S. baicalensis*, *H. cordata*, and *I. indigotica* in NRICM101 demonstrated the ability to fight against SARS-CoV-2 infection. The developed pseudovirus system was used to detect the inhibitory effects of *S. baicalensis*, *H. cordata*, and *I. indigotica* on the interaction between viral spike protein and the hACE2 receptor. First, we analyzed the effect of different concentrations of *S. baicalensis*, *H. cordata*, and *I. indigotica* on cell viability using an MTT assay. The results showed that the cell viability slightly decreased with *S. baicalensis* and *H. cordata* at 1,000 μg/mL (**Figure 3a** and **3b**). When the cells were treated with 1,000 μg/mL *I. indigotica*, no mortality was observed (**Figure 3c**). These substances showed low cytotoxicity

 doi:10.20944/preprints202401.2061.v1

and safety within a certain concentration range. Collectively, the cell viability and efficacy data for the pseudovirus indicated that *S. baicalensis* (250 μg/mL) showed significantly effective inhibitory efficacy compared with those of *H. cordata* and *I. indigotica* (250 μg/mL). This result indicated that *S. baicalensis* plays an important role in NRICM101 blocking the interaction between the viral spike protein and the hACE2 receptor.

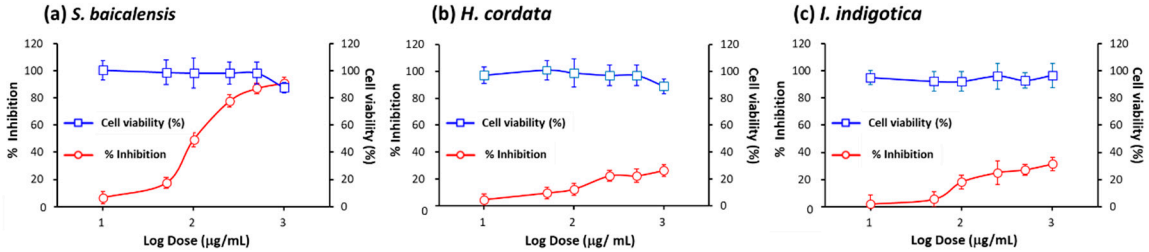

Figure 3. Assessment of inhibitory efficacy of *S.* baicalensis, *H.* cordata, and *I.* indigotica against SARS-CoV-2 BA.2 spike pseudovirus infection. The inhibitory efficacy and cell viability of *S. baicalensis* (**a**), *H. cordata* (**b**), and *I. indigotica* (**c**) were quantified using a Synergy HT multimode microplate reader at final concentrations of 0, 10, 100, 250, 500, and 1,000 μg/mL for 24 h. All values are expressed as mean ± SD for each group (n = 5).

2.4. Identification of active ingredients in S. baicalensis

S. baicalensis effectively inhibited the interaction between the viral spike protein and hACE2. The relative inhibition ratio was determined using the developed pseudovirus system. Then, we focused on finding the biologically active components in *S. baicalensis*. We used LC-MS to gradually separate the compounds in *S. baicalensis* and track the biologically active ingredients. According to the retention time (RT) in the ESI/MS-negative-mode mass spectra, the 10 major active ingredients in *S. baicalensis* were identified: chrysin 6-C-arabinoside-8-C-glucoside, chrysin 6-C-glucoside-8-C-arabinoside, scutellarin, quercetin, baicalin and wogonin 7-O-glucuronide (wogonoside), oroxylin A-7-O-glucuronide (oroxyloside), rhamnocitrin, baicalein, and oroxylin A (**Figure 4a**). Moreover, pure baicalein was the most strongly detected in the analysis (**Figure 4b**), and the intensity of pure baicalin in *S. baicalensis* was the second strongest active ingredient (**Figure 4c**). According to the experimental results, we investigated the efficacy of baicalein and baicalin in inhibiting pseudovirus infection.

 doi:10.20944/preprints202401.2061.v1

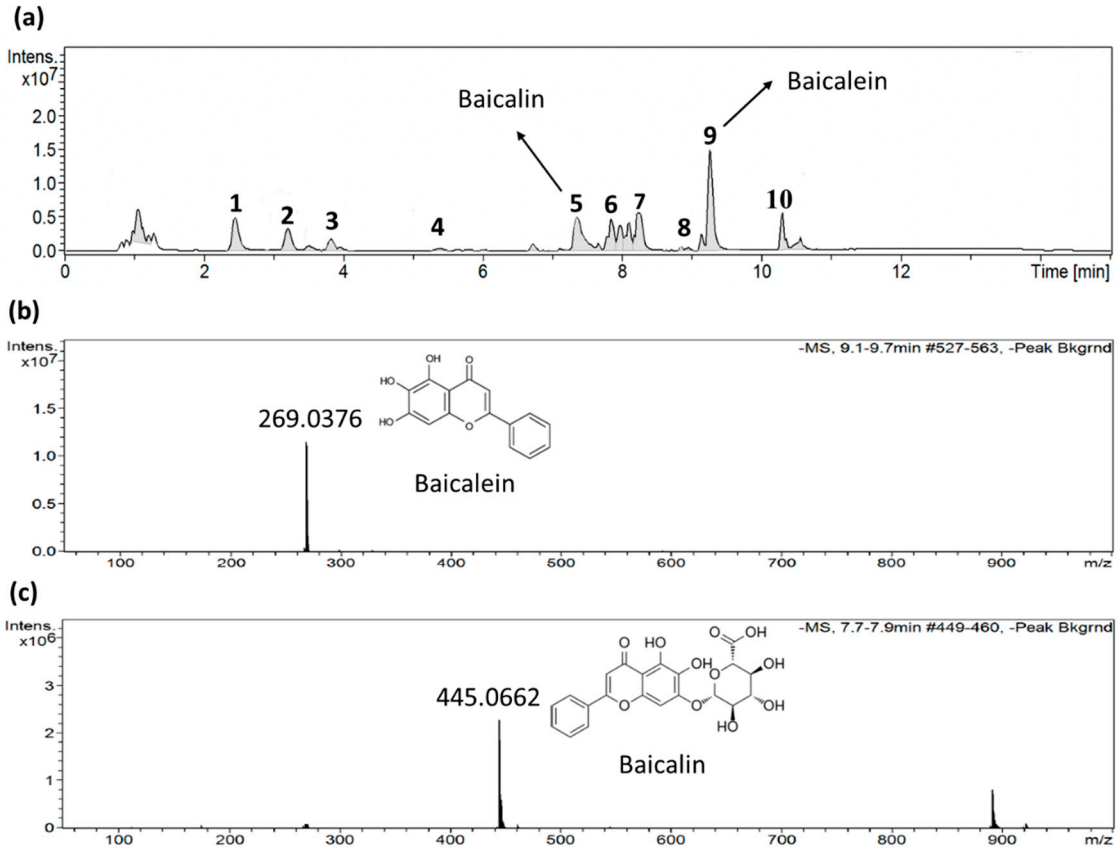

Figure 4. LC-MS fingerprint profiles of *S. baicalensis* extract. LC profiles of the TCM compound were obtained with an Impact HD Q-TOF mass spectrometer through ESI(+)(-)MS experiments. Ten major constituents were found in the *S. baicalensis* extract (**a**). ESI/MS negative-mode mass spectra fingerprint of baicalein (**b**). ESI/MS negative-mode mass spectra fingerprint of baicalin (**c**).

2.5. Baicalein and baicalin inhibition of Omicron spike pseudovirus infection

Based on the results from the LC-MS analysis, we further examined the inhibitory activities of baicalein and baicalin at concentrations of 1, 5, 10, 25, 50, 75, and 100 μM. The pseudovirus system was used to elucidate the affinity among the spike protein, hACE2, baicalein, and baicalin. To better understand the inhibitory activities, we examined baicalein and baicalin pretreated with SARS-CoV-2 spike pseudovirus (Group PV) and HEK293T-hACE2 cells (Group PC) for 4 h (**Figure 5a**). Baicalein showed an IC_{50} of 43.98 μM in Group PV group and an IC_{50} of 56.43 μM in Group PC (**Figure 5b**). Baicalin showed an IC_{50} of 103.71 μM in Group PV and an IC_{50} of 83.44 μM in Group PC (**Figure 5c**). The results indicated that both baicalein and baicalin effectively inhibited the entry of the spike pseudovirus. Additionally, these results showed that the inhibitory efficacy of baicalein can be strengthened via pretreatment with pseudovirus. On the contrary, baicalin had a stronger inhibitory efficacy when pretreated with HEK293T-hACE2 cells.

 doi:10.20944/preprints202401.2061.v1

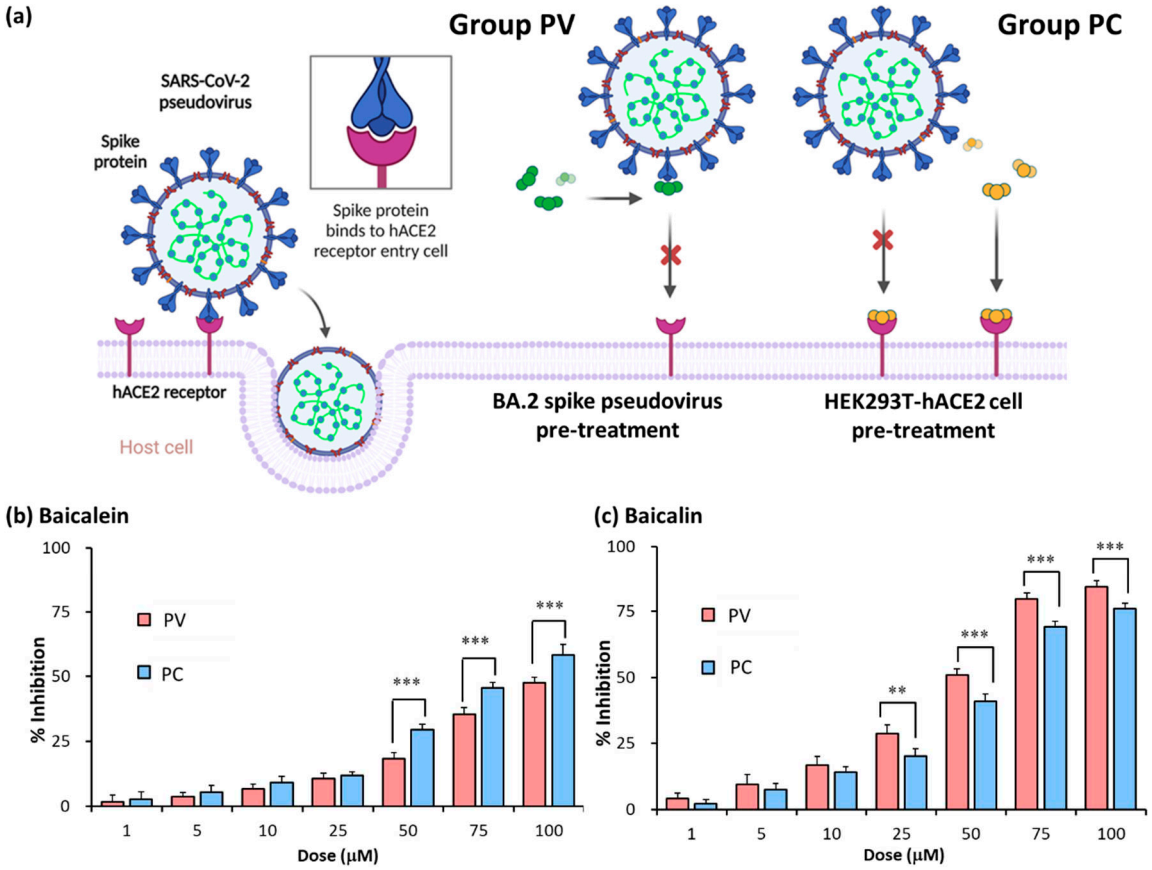

Figure 5. Assessment of inhibitory efficacy of baicalein and baicalin of SARS-CoV-2 BA.2 spike pseudovirus infection. Experimental scheme indicating the pseudovirus pretreatment (Group PV) and the cell pretreatment (Group PC) of baicalein and baicalin (**a**). The inhibitory efficacy of baicalein pretreated with SARS-CoV-2 BA.2 spike pseudovirus and HEK29T-hACE2 cells was quantified using a Synergy HT multimode microplate reader (**b**). The inhibitory efficacy of baicalin pretreated with SARS-CoV-2 BA.2 spike pseudovirus and HEK29T-hACE2 cells was quantified with a Synergy HT multimode microplate reader (**c**). All values are expressed as mean ± SD for each group (n = 5). The statistical comparison between groups was conducted using Student's t-test; ** $p < 0.01$ and *** $p < 0.001$ vs. PV group.

2.6. Synergistic effect of baicalein and baicalin on pseudovirus infection inhibition

To identify an effective strategy for SARS-CoV-2 prevention targeting the interaction of mutated spike proteins with hACE2, we investigated the synergistic effect between baicalein and baicalin. We combined the baicalein pretreated for 4 h with pseudovirus and baicalin pretreated with HEK293T-hACE2 cells at final concentrations of 0, 1, 5, 10, 25, 50, 75, and 100 μM. We used the zero-interaction potency (ZIP) synergy score map to visualize the synergistic patterns between baicalein and baicalin. As shown in **Figure 6a**, the inhibitory value for the responses varied at different doses, suggesting that not all scores were equally important. High delta scores (> 5) were also confirmed for various combinations of baicalein and baicalin. When 25 μM baicalein was combined with 75 μM baicalin, 87.9% virus inhibition was attained. However, the inhibition was only 84.3% for 100 μM baicalein. The interaction of baicalein and baicalin was synergistic over the dose–response matrix, leading to a maximal combination effect close to 100% cell inhibition at higher concentrations of both drugs (**Figure 6b**). The average delta score for the confirmed combinations was 13.373, which was significantly higher than the average synergy score (=10) of the combinations. Taken together, the interaction results indicated that the combination of baicalein and baicalin could produce a stronger effect than individual compounds while maintaining acceptable doses and limiting side effects.

 doi:10.20944/preprints202401.2061.v1

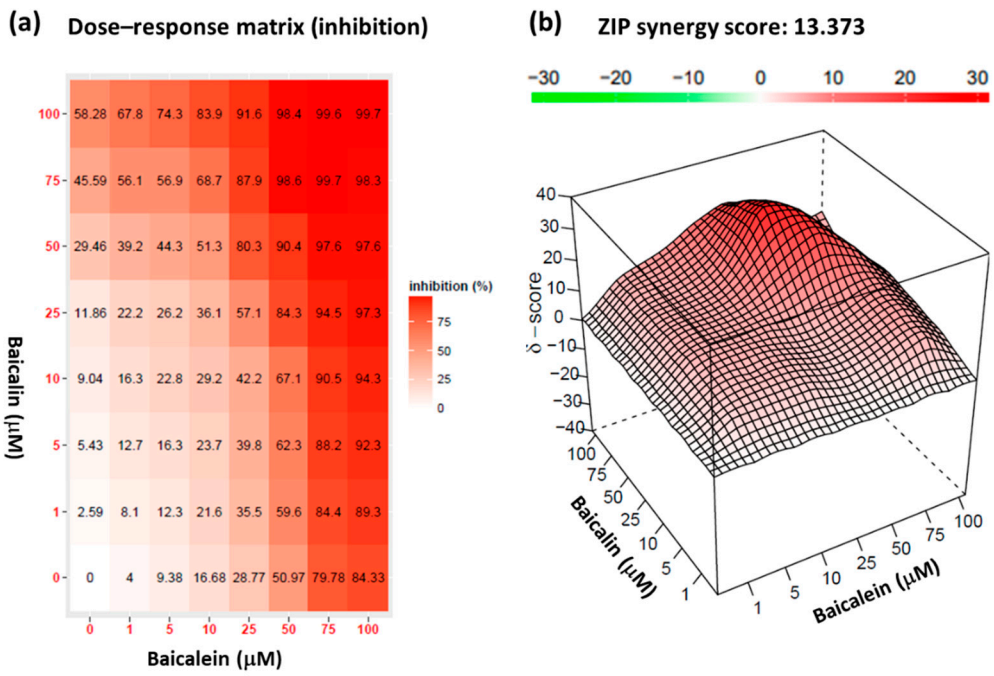

Figure 6. Synergism between baicalin and baicalein. Dose–response map for a synergistic drug combination (baicalein and baicalin) (**a**). ZIP synergy score map for the same drug combinations (**b**). The interaction results are shown in both 2D and 3D. δ, excess % inhibition beyond the expectation predicted with the ZIP model; Δ, average δ scores over the dose–response matrix.

3. Discussion

TCM is an important resource of bioactive natural products that are widely used for the treatment of hepatitis, atherosclerosis, hypertension, hyperlipidemia, type 2 diabetes, and respiratory disorders [30-32]. *S. baicalensis* has been widely used in TCM for COVID-19 treatment. *S.* baicalensis is effective at inhibiting SARS-CoV-2 infection as a screening object [33-36]. However, the major components of *S. baicalensis* and their mechanisms in this effect remain to be explored.

The inhibitory effects of the selected TCM on viral entry, a pivotal step in virus infection, were determined using the pseudovirus system. *S. baicalensis* was the most effective in inhibiting pseudovirus infection, especially against the Omicron spike pseudovirus (**Figure 2**). Baicalein and baicalin are the main components of *S. baicalensis* (**Figure 3**), which both inhibit SARS-CoV-2 infection of cells via the hACE2 receptor (**Figure 4**). Baicalein prefers blocking the viral spike protein, whereas baicalin prefers blocking hACE2 (**Figure 5**). In addition, the interaction results indicated the efficacy of the combination of baicalein and baicalin in targeting the interaction between the spike protein and ACE2 (**Figure 6**).

TCM has been widely applied to treat COVID-19, being found to alleviate the symptoms of the disease, delay the progression of mild to severe disease, and increase cure rates [35, 36]. NRICM101 has demonstrated both antiviral and anti-inflammatory effects against COVID-19 since 2020 [16, 23], showing promise as a multitarget agent for the prevention and treatment of COVID-19 [16]. However, given the high mutation rate of the virus and the increased risk of immune viral escape, emerging SARS-CoV-2 variants have exhibited antiviral resistance, allowing the viruses to escape the immune system [37, 38]. Thus, this study aimed to explore the more effective components in the TCM that are used to treat SARS-CoV-2 variants by targeting the interaction of mutated spike proteins and hACE2.

Some of the TCM of NRICM101 have *anti-inflammatory effects, such as H.* cordata and *I. indigotica* [39, 40]; some have antioxidant effects, such as mulberry leaf [41]. *S. baicalensis* can inhibit the activation of 3C-like protease (3CLpro) and the replication of SARS-CoV-2 [22, 42]. Specifically, *S. baicalensis* has the potential to prevent SARS-CoV-2 entry into host cells by blocking the viral spike

 doi:10.20944/preprints202401.2061.v1

protein or the hACE2 receptor [42] and reducing the expression level of hACE2 to decrease the interaction of the viral spike protein with its hACE2 receptor [43]. However, the component that directly interrupts the interaction of the viral spike protein with the host's hACE2 is still unclear. To determine the composition of *S. baicalensis*, we performed LC-MS fingerprint analysis to reveal the active ingredients, which include baicalin, baicalein, wogonin, wogonoside, and oroxylin A. According to the LC-MS data, baicalein and baicalein were the main active competent in *S. baicalensis* (**Figure 4**).

S. baicalensis dose-dependently prevents spike–hACE2 interaction (**Figure 3**). This means that baicalein and baicalein possibly play crucial roles in the treatment and prevention of virus invasion. Baicalein and baicalin have various pharmacological effects against COVID-19, including anti-inflammatory, antiviral, antibacterial, hepatoprotective, and choleretic activities [44, 45]. Baicalein and baicalin were able to participate in the RNA replication process of the virus [46, 47] and inhibit the crucial 3CLpro of SARS-CoV-2 [48, 49]. In addition, baicalein and baicalin prevent SARS-CoV-2 entry into host cells by blocking viral spike protein and reducing the hACE2 expression level [43]. In our study, we confirmed that baicalein and baicalein could disrupt hACE2–spike interaction with the pseudovirus system.

Baicalein forms a stable hydrogen bond with the spike protein Gln498, a key amino acid residue in the binding of spike protein to the hACE2 receptor [24]. The results of a molecular docking analysis showed that baicalin strongly binds with hACE2 with a binding energy of –8.46 kcal/mol via binding to the residues Asn149, Arg273, and His505 of hACE2 [50]. In this study, the in vitro pseudovirus results support the published bioinformatics and molecular interaction results. Baicalein had a stronger inhibitory efficacy when pretreated with the SARS-CoV-2 spike pseudovirus. Baicalin had a higher inhibitory efficacy when pretreated with HEK293T-hACE2 cells (Figure 5). Based on the above, we consider baicalein a potential spike blocker and baicalin as an ACE2 blocker for blocking the interaction of viral spike protein and hACE2. According to the results of a pharmacological effect assay and dynamics simulations, Song et al. [51] reported that baicalein can simultaneously interfere with multiple targets and in the interaction between the spike protein and hACE2 receptor. Baicalein may be a potential candidate for treatment of SARS-CoV-2 and its variants, especially Omicron. For the original hACE2/spike-RBD, baicalein interacts with the active site through three hydrogen bonds with Asn33, Tyr505, and Arg393, showing van der Waals interactions with Asp30 and Glu37 of the spike protein. For delta hACE2/S-RBD, Song et al. [47] found that baicalein interacts with residues Asp30, Lys26, Leu29, Asn33, Glu96, Pro389, Gln388, Ala387, Thr92, Val93, and Asn90. Shakhsi-Niaei et al. [51] reported that baicalin is a candidate to occupy hACE2 and inhibit viral RBD binding., i.e., baicalin is a stronger inhibitor of the SARS-CoV-2 binding site of ACE2. The results of this molecular simulating study showed that baicalin interacts with the active site through three hydrogen bonds with A396, E208, and D206. Many scientists are studying the possibility of developing a molecule, such as baicalein and baicalin from *S. baicalensis*, as effective antiviral drugs [24, 33, 50-52].

To identify an effective strategy for SARS-CoV-2 prevention, we investigated the synergistic effects between the baicalein and baicalin. An efficient experimental–computational approach was used to identify most potent synergistic and antagonistic combinations [31, 53]. In this study, we systematically conducted combination experiments to assess drug interactions using a ZIP model to capture shifts in interaction potency [54]. To conduct a more systematic analysis of the whole dose–response matrix, we implemented a surface plot approach based on delta scoring to visualize the range of drug interactions over all tested dose pairs. The interaction results indicated that the combination of baicalein and baicalin produced stronger effects than the individual compounds while maintaining acceptable doses and limited side effects. Further studies are required to analyze these compounds and their structurally related derivatives. The increased specificity of combinations over single agents has implications for the development of an anti-SARS-CoV-2 drug candidate for further preclinical studies.

4. Materials and Methods

4.1. Chemicals and reagents

 doi:10.20944/preprints202401.2061.v1

Anti-ACE2 polyclonal antibody [N1N2], anti-SARS-CoV/SARS-CoV-2 (COVID-19) spike monoclonal antibody [1A9], goat anti-rabbit IgG antibody, and goat antimouse IgG antibody were purchased from Genetex (Irvine, CA, USA). Anti-β-actin rabbit monoclonal antibody was bought from Cell Signaling Technology (Danvers, MA, USA). Baicalein (5,6,7-trihydroxyflavone) and baicalin (5,6,7-trihydroxyflavone-7-O-β-D-glucuronide) were purchased from MedChemExpress (Princeton, NJ, USA).

4.2. Cell culture and cell viability assay

The human embryonic kidney 293T cell line (HEK293T) was obtained from American Type Culture Collection (ATCC; Manassas, VA, USA). HEK293T cells stably expressing hACE2, named the HEK293T-hACE2 cell line, were obtained from the Food Industry Research and Development Institute (Hsinchu, Taiwan). HEK293T and HEK293T-hACE2 cells were cultured in Dulbecco's modified Eagle's medium (DMEM) with 10% fetal bovine serum (FBS) and maintained in a humidified atmosphere of 5% CO_2 at 37 °C.

For the cell viability assay, the HEK293T-hACE2 cells were seeded in 96-well plates and incubated for 24 h before starting the experiment. The cells were cultured with treatment for 24 h. After the treatment, 10 µL of 3-(4,5-Dimethyl-2-thiazolyl)-2,5-diphenyl-2H-tetrazolium bromide (MTT) solution was added to each well for 4 h. Then, all fluid in the wells was aspirated, and 100 µL of DMSO was added to each well, which was then shaken for 10 min. After, the GPF fluorescence was detected using a Synergy HT multimode microplate reader (BioTek Instruments, Winooski, VT, USA), and absorbance was detected at 540 nm.

4.3. Pseudovirus system

As shown in Figure 7, the lentivirus packaging system was used to produce SARS-CoV-2 spike pseudovirus. Three vectors were chosen for construction: pCMVΔR8.91, pLAS2.1w.PeGFP-I2-Puro (RNAiCore, Taipei, Taiwan), pcDNA3.1-SARS2-Spike, and pcDNA3.3_SARS2_Omicron BA.2 (Addgene, Watertown, MA, USA). HEK293T was seeded onto a 24-well plate and cultured for 24 h. Then, 15 µg of plasmid DNA (Ration of transfer vector: packaging vector: envelope vector = 10:9:1) and Lipofectamine 2000 Transfection Reagent (Thermo Fisher Scientific, Waltham, MA, USA) were co-transfected into HEK293T cells. The pseudovirus was harvested 72 h after transfection for the experiments. The HEK293T-hACE2 cells were infected with the pseudovirus for 24 h at 37 °C. After the incubation, the virions were removed, and the infected cells were cultured in fresh medium for another 72 h. The GFP of the cells was observed via microscopy at 72 h after infection. Additionally, the cells were collected 72 h after infection to analyze the GFP intensity using a Synergy HT multimode microplate reader (BioTek Instruments).

 doi:10.20944/preprints202401.2061.v1

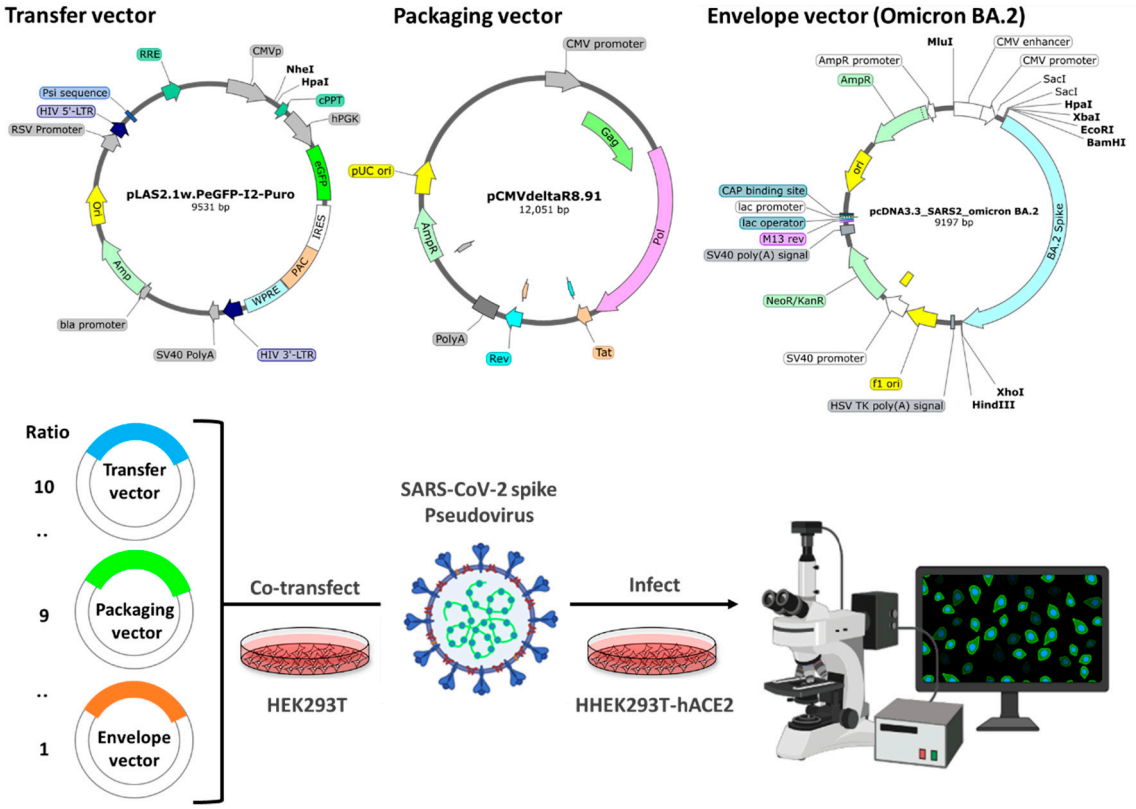

Figure 7. Schematic representation of the SARS-CoV-2 spike pseudovirus system.

4.4. Pseudovirus infection inhibition assay

HEK293T-hACE2 cells were seeded into 24-well plates (5×10^4 cells/well) 24 h before the experiment. The blocker molecules or TCM extracts were co-incubated with the pseudovirus for 24 h at 37°C. The next day, the pseudovirus was removed, and cells were cultured in the fresh medium for another 72 h. To evaluate the inhibition efficiency, the GFP intensity was measured at 72 h after infection, and the treatment groups were compared with the control group.

4.5. Protein extraction

The cell samples derived from HEK293T and HEK293T-hACE2 cells were collected and then homogenized with PRO-PREPTM protein extraction solution (INTERCHIM, San Diego, CA, US). The cell lysate was centrifuged at 13,000x g for 10 min, and the supernatants were collected and preserved. We quantified the total protein in the cell lysate using a Bradford dye binding assay (Bio-Rad Laboratories, Hercules, CA, USA) with bovine serum albumin as the standard. The cell protein lysate was aliquoted and stored at -25°C until further use.

4.6. Western blot

The samples containing 10 μg of protein with 4X protein dye was loaded onto 10% SDS-PAGE gels. After electrophoretic separation, polyvinylidene fluoride membranes (PVDF; Bio-Rad Laboratories) were soaked in methanol for 1 min. Then, the protein sample was transferred to a PVDF membrane via wet electroblotting. To block nonspecific binding, the PVDF membranes were treated with a blocking solution consisting of 5% nonfat milk in Tris-buffered saline. The primary antibodies used for ACE2, spike protein, and β-actin were diluted to 1:1,000. The secondary antibodies were diluted to 1:4,000. The substrate containing secondary antibodies was conjugated horseradish peroxidase (HRP), and enhanced chemiluminescent (ECL) was used to detect HRP (GeneTex). The target location of the bands was detected based on protein weight using iBright Imaging Systems

 doi:10.20944/preprints202401.2061.v1

(Thermo Fisher Scientific). The band's intensity was quantified using ImageJ. The expression levels of hACE2 and spike proteins were calculated and compared with that of β-actin for every sample.

4.7. Extraction of each TCM

Dried Scutellaria root, heartleaf, and Indigowoad root (60 g) were purchased from a Chinese herbal store in Taipei, Taiwan, and were authenticated by Dr. Pei-Ching Wu at the Department of Chinese Medicine, China Medical University Hospital, Taichung, Taiwan. The herbs were chopped and boiled in 600 mL of water for 30 min and simmered until the decoction reduced to 100 mL. The supernatant was collected and filtered through a 0.22 μm PVDF filter. The filtered solution was aliquoted and stored at -80°C for 1 day. Then, the filtered solution was dried in a freeze-dryer for 4–5 days to yield a crude extract. The lyophilized powder of the extracts (20 mg) was dissolved in 1 mL of water as a stock solution (20 mg/mL). All the tested solutions were filtered through a 0.22 μm PVDF filter before use.

4.8. LC-MS analyses

LC-MS analyses were conducted by the Center for Advanced Instrumentation and the Department of Applied Chemistry at National Yang Ming Chiao Tung University, Hsinchu, Taiwan. Ultra-performance liquid chromatography (UPLC) of the sample solutions (pH 7.5) was performed via direct infusion (2 μL). High-resolution electrospray mass spectrometry (HRESI-MS) was conducted with an Impact HD Q-TOF mass spectrometer (Bruker, Karlsruhe, Germany) that was equipped with an electrospray ionization (ESI) source in positive-ion mode. The detailed ESI (+) parameters were as follows: ion spray voltage was 4.5 kV; the capillary temperature was 200°C; the sheath gas flow rate was 6 L/min. The mass spectra were collected over the mass range of m/z 50-1,500 at a resolving power of 40,000. The final data were analyzed using Compass DataAnalysis 4.1 (Bruker). A 20 mg/mL solution of the compound was analyzed.

4.9. Synergy scoring and detection

The synergic effect of baicalein and baicalin was predicted using SynergyFinder 3.0, which is a web application for analyzing dose–response matrix data of drug combinations [55]. Cells were treated with baicalein at a final concentration of 1, 5, 10, 25, 50, 75, or 100 μM and with baicalin at 1, 5, 10, 25, 50, or 100 μM for 4 h. The cells were collected 72 h after infection to analyze the GFP intensity using a Synergy HT multimode microplate reader. The Bliss independence model was used as the primary method to score drug combination synergy in the datasets; although the results are based on the Loewe additivity, the results of the highest single agent (HSA) and ZIP model are additionally shown for providing complementary information from various models [56]. A synergy score value >10 is considered synergistic, a score of between −10 and +10 is considered additive, and a synergy score <−10 is considered antagonistic [57].

4.10. Statistical analysis

All values are expressed as the mean ± standard deviation (SD; n=3 for each treatment). The data were compared using Student's t-test to evaluate differences between groups. p-value ≤ 0.05, p-value ≤ 0.01, and p-value ≤ 0.001 were considered statistically significant.

5. Conclusions

This study systematically evaluated the antiviral entry activity of TCM using a SARS-CoV-2 spike pseudovirus system. We identified two natural components, baicalein and baicalin, as novel antiviral therapeutic candidates that for blocking the interaction of the viral spike protein with the host hACE2, thereby inhibiting SARS-CoV-2 infection. Our results warrant further evaluation and characterization to work toward the development of a drug for COVID-19 treatment. Baicalein had a stronger binding affinity to the viral spike protein, and baicalin had a stronger binding affinity to the hACE2 receptor. In addition, the drug synergy results indicated that the combination of baicalein and

baicalin produced a stronger effect than either compound alone while maintaining acceptable doses and limited side effects. Further studies rare need to analyze these compounds and their structurally related derivatives, alone as well as in combination with effective nucleoside analogs for the development of novel anti-SARS-CoV-2 drug candidates for further preclinical studies. The detailed mechanisms and dynamic reactions of baicalein and baicalin in antiviral infection remain to be explored.

6. Patents

Author Contributions: Conceptualization, C.-H.L. and C.-S.L.; writing-original draft preparation, C.-H.L., H.-J.C. and M.-W.L.; writing-review and editing, C.-H.L., C.-H. L.; M.-W.L. and C.-S.L.; Investigation, C.-H.L., H.-J.C., and X.-R.Y.; Supervision, C.-S.L. All authors have read and agreed to the published version of the manuscript.

Funding: This work received no external funding.

Institutional Review Board Statement: Not applicable.

Informed Consent Statement: All data in this study were obtained from published material in scientific journals, referenced in the paper, and can be obtained by any individual with access.

Data Availability Statement: The data presented in this study are available upon request from the corresponding author.

Acknowledgments: This work was supported by the grants of NSTC 110-2312-B-A49-001-MY3, NSTC 112-2811-B-A49-501, NSTC 112-2811-B-A49-503, NSTC 112-2321-B-A49-018, NSTC 112-2321-B-A49-005, and NSTC 112-2221-E-033-013-MY3 from the National Science and Technology Council (NSTC), Taiwan. This work was also financially supported by the "Center for Intelligent Drug Systems and Smart Bio-devices (IDS^{2}B)" from The Featured Areas Research Center Program within the framework of the Higher Education Sprout Project of the National Yang Ming Chiao Tung University and Ministry of Education (MOE), Taiwan.

Conflicts of Interest: All of the authors declare no competing conflict of interest.

References

1. Wang, M.; Cao, R.; Zhang, L.; Yang, X.; Liu, J.; Xu, M.; Shi, Z.; Hu, Z.; Zhong, W.; Xiao, G. Remdesivir and chloroquine effectively inhibit the recently emerged novel coronavirus (2019-nCoV) *in vitro*. *Cell Res* **2020**, 30, 269-271.
2. Callaway, E. Beyond Omicron: what's next for COVID's viral evolution. *Nature* **2021**, 600, 204-207.
3. Pustake, M.; Tambolkar, I.; Giri, P.; Gandhi, C. SARS, MERS and CoVID-19: An overview and comparison of clinical, laboratory and radiological features. *J Family Med Prim Care* **2022**, 11, 10-17
4. Saldivar-Espinoza, B.; Garcia-Segura, P.; Novau-Ferré, N.; Macip, G.; Martínez, R.; Puigbò, P.; Cereto-Massagué, A.; Pujadas, G.; Garcia-Vallve, S. The Mutational Landscape of SARS-CoV-2. *Int J Mol Sci* **2023**, 24, 9072.
5. Chan, J.F.; Kok, K.H.; Zhu, Z.; Chu, H.; To, K.K.; Yuan, S.; Yuen, K.Y. Genomic characterization of the 2019 novel human-pathogenic coronavirus isolated from a patient with atypical pneumonia after visiting Wuhan. *Emerg Microbes Infect* **2020**, 9, 221-236.
6. Chatterjee, S.; Bhattacharya, M.; Nag, S.; Dhama, K.; Chakraborty, C. A detailed overview of SARS-CoV-2 omicron: its sub-variants, mutations and pathophysiology, clinical characteristics, immunological landscape, immune escape, and therapies. *Viruses* **2023**, 15, 167.
7. Lamkiewicz, K.; Esquivel Gomez, L.R.; Kühnert, D.; Marz, M. Genome structure, life cycle, and taxonomy of coronaviruses and the evolution of SARS-CoV-2. In Viral Fitness and Evolution: Population Dynamics and Adaptive Mechanisms; *Springer*: **2023**; pp. 305-339.
8. Hirano, T.; Murakami, M. COVID-19: a new virus, but a familiar receptor and cytokine release syndrome. *Immunity* **2020**, 52, 731-733.
9. Yang, L.; Li, J.; Guo, S.; Hou, C.; Liao, C.; Shi, L.; Ma, X.; Jiang, S.; Zheng, B.; Fang, Y. SARS-CoV-2 variants, RBD mutations, binding affinity, and antibody escape. *Int J Mol Sci* **2021**, 22, 12114.
10. Borkotoky, S.; Dey, D.; Hazarika, Z. Interactions of angiotensin-converting enzyme-2 (ACE2) and SARS-CoV-2 spike receptor-binding domain (RBD): a structural perspective. *Mol Biol Rep* **2023**, 50, 2713-2721.
11. Reuter, N.; Chen, X.; Kropff, B.; Peter, A.S.; Britt, W.J.; Mach, M.; Überla, K.; Thomas, M. SARS-CoV-2 Spike Protein Is Capable of Inducing Cell–Cell Fusions Independent from Its Receptor ACE2 and This Activity Can Be Impaired by Furin Inhibitors or a Subset of Monoclonal Antibodies. *Viruses* **2023**, 15, 1500.
12. Marshall, A.C. Traditional Chinese medicine and clinical pharmacology; *Springer*: **2020.** 455–482.

13. Lyu, M.; Fan, G.; Xiao, G.; Wang, T.; Xu, D.; Gao, J.; Ge, S.; Li, Q.; Ma, Y.; Zhang, H. *Acta Pharm Sin B* **2021**, 11, 3337-3363.
14. Zhao, Z.; Li, Y.; Zhou, L.; Zhou, X.; Xie, B.; Zhang, W.; Sun, J. Prevention and treatment of COVID-19 using Traditional Chinese Medicine: A review. *Phytomedicine* **2021**, 85, 153308.
15. Martín Giménez, V.M.; Modrego, J.; Gómez-Garre, D.; Manucha, W.; de Las Heras, N. Gut microbiota dysbiosis in COVID-19: Modulation and approaches for prevention and therapy. *Int J Mol Sci* **2023**, 24, 12249.
16. Tsai, K.C.; Huang, Y.C.; Liaw, C.C.; Tsai, C.I.; Chiou, C.T.; Lin, C.J.; Wei, W. C.; Lin, S. J.; Tseng, Y.H.; Yeh, K.M.; et al. A traditional Chinese medicine formula NRICM101 to target COVID-19 through multiple pathways: A bedside-to-bench study. *Biomed Pharmacother* **2021**, 133, 111037.
17. Chang, C.H.; Peng, W.Y.; Lee, W.H.; Lin, T.Y.; Yang, M.H.; Dalley, J.W.; Tsai, T.H. Biotransformation and brain distribution of the anti-COVID-19 drug molnupiravir and herb-drug pharmacokinetic interactions between the herbal extract *Scutellaria* formula-NRICM101. *J Pharm Biomed Anal* **2023**, 115499.
18. Lin, C.H.; Chen, Y.J.; Lin, M.W.; Chang, H.J.; Yang, X.R.; Lin, C.S. ACE2 and a Traditional Chinese Medicine Formula NRICM101 Could Alleviate the Inflammation and Pathogenic Process of Acute Lung Injury. *Medicina* **2023**, 59, 1554.
19. Wang, M.; Tao, L.; Xu, H. Chinese herbal medicines as a source of molecules with anti-enterovirus 71 activity. *Chin Med,* **2016**, 11, 1-26.
20. Zhao, T.; Tang, H.; Xie, L.; Zheng, Y.; Ma, Z.; Sun, Q.; Li, X. *Scutellaria baicalensis* Georgi. (Lamiaceae): a review of its traditional uses, botany, phytochemistry, pharmacology and toxicology. *J Pharm Pharmacol* **2019**, 71, 1353-1369.
21. Chen, Q.; Lan, H.Y.; Peng, W.; Rahman, K.; Liu, Q.C.; Luan, X.; Zhang, H. *Isatis indigotica*: a review of phytochemistry, pharmacological activities and clinical applications. *J Pharm Pharmacol* **2021**, 73, 1137-1150.
22. Kaul, R.; Paul, P.; Kumar, S.; Büsselberg, D.; Dwivedi, V.D.; Chaari, A. Promising antiviral activities of natural flavonoids against SARS-CoV-2 targets: systematic review. *Int J Mol Sci* **2021**, 22, 11069.
23. Liu, H.; Ye, F.; Sun, Q.; Liang, H.; Li, C.; Li, S.; Lu, R.; Huang, B.; Tan, W.; Lai, L. *Scutellaria baicalensis* extract and baicalein inhibit replication of SARS-CoV-2 and its 3C-like protease *in vitro*. *J Enzyme Inhib Med Chem* **2021**, 36, 497-503.
24. Yang, Y.; Islam, M.S.; Wang, J.; Li, Y.; Chen, X. Traditional Chinese Medicine in the Treatment of Patients Infected with 2019-New Coronavirus (SARS-CoV-2): A Review and Perspective. *Int J Biol Sci* **2020**, 16, 1708-1717.
25. Ghosh, R.; Chakraborty, A.; Biswas, A.; Chowdhuri, S. Depicting the inhibitory potential of polyphenols from Isatis indigotica root against the main protease of SARS CoV-2 using computational approaches. *J Biomol Struct Dyn* **2022**, 40, 4110-4121.
26. Thoene, J.; Gavin, R.F.; Towne, A.; Wattay, L.; Ferrari, M.G.; Navarrete, J.; Pal, R. In vitro activity of cysteamine against SARS-CoV-2 variants. *Mol Genet Metab*, **2022**, 137, 192–200.
27. Alonzi, T.; Aiello, A.; Repele, F.; Falasca, L.; Francalancia, M.; Garbuglia, A. R.; Delogu, G.; Nicastri, E.; Piacentini, M.; Goletti, D.; et al. Cysteamine exerts in vitro antiviral activity against the SARS-CoV-2 Delta and Omicron variants. *Cell Death Discov*, **2020**, 8, 288.
28. Wang, G.; Yang, M.L.; Duan, Z.L.; Liu, F.L.; Jin, L.; Long, C.B.; Zhang, M.; Tang, X. P.; Xu, L.; Li, Y.C.; et al. Dalbavancin binds ACE2 to block its interaction with SARS-CoV-2 spike protein and is effective in inhibiting SARS-CoV-2 infection in animal models. *Cell Res*, **2021**, 31, 17–24.
29. Hoffmann, M.; Jin, Y.; Pöhlmann, S. Dalbavancin: novel candidate for COVID-19 treatment. *Cell Res*, **2021**, 31, 243–244.
30. Fang, P.; Yu, M.; Shi, M.; Bo, P.; Gu, X.; Zhang, Z. Baicalin and its aglycone: a novel approach for treatment of metabolic disorders. *Pharmacol Rep* **2020**, 72, 13-23.
31. Liang, S.; Deng, X.; Lei, L.; Zheng, Y.; Ai, J.; Chen, L.; Xiong, H.; Mei, Z.; Cheng, Y.-C.; Ren, Y. The comparative study of the therapeutic effects and mechanism of baicalin, baicalein, and their combination on ulcerative colitis rat. *Front Pharmacol* **2019**, 10, 1466.
32. Dinda, B.; Dinda, S.; DasSharma, S.; Banik, R.; Chakraborty, A.; Dinda, M. Therapeutic potentials of baicalin and its aglycone, baicalein against inflammatory disorders. *Eur J Med Chem* **2017**, 131, 68-80.
33. Song, J.W.; Long, J.Y.; Xie, L.; Zhang, L.L.; Xie, Q.X.; Chen, H.J.; Deng, M.; Li, X.F. Applications, phytochemistry, pharmacological effects, pharmacokinetics, toxicity of *Scutellaria baicalensis* Georgi. and its probably potential therapeutic effects on COVID-19: a review. *Chin Med* **2020**, 15, 1-26.
34. Boozari, M.; Hosseinzadeh, H. Natural products for COVID-19 prevention and treatment regarding to previous coronavirus infections and novel studies. *Phytother Res* **2021**, 35, 864-876.
35. Jia, K.; Li, Y.; Liu, T.; Gu, X.; Li, X. New insights for infection mechanism and potential targets of COVID-19: Three Chinese patent medicines and three Chinese medicine formulas as promising therapeutic approaches. *Chin Herb Med*. **2023**, 15, 157-168.

36. Fuzimoto, A.D.; Isidoro, C. The antiviral and coronavirus-host protein pathways inhibiting properties of herbs and natural compounds-Additional weapons in the fight against the COVID-19 pandemic? *J Tradit Complement Med* **2020**, 10, 405-419.
37. Carabelli, A.M.; Peacock, T.P.; Thorne, L.G.; Harvey, W.T.; Hughes, J.; 6, C.-G.U.C.d.S.T.I.; Peacock, S.J.; Barclay, W.S.; de Silva, T.I.; Towers, G.J. SARS-CoV-2 variant biology: immune escape, transmission and fitness. *Nat Rev Microbiol* **2023**, 21, 162-177.
38. Fan, Y.; Li, X.; Zhang, L.; Wan, S.; Zhang, L.; Zhou, F. SARS-CoV-2 Omicron variant: recent progress and future perspectives. *Signal Transduct Target Ther* **2022**, 7, 141.
39. Chun, J.M.; Kim, H.S.; Lee, A.Y.; Kim, S.H.; Kim, H.K. Anti-Inflammatory and Antiosteoarthritis Effects of Saposhnikovia divaricata ethanol Extract: *In Vitro* and *In Vivo* Studies. Evid Based Complement *Alternat Med 2016*, **2016**, 1984238.
40. Laldinsangi, C. The therapeutic potential of *Houttuynia cordata*: A current review. *Heliyon* **2022**, 8, e10386
41. Zhu, Y.; Han, Y.; Wang, W.; Liang, G.; Qi, J. Mulberry leaves attenuate D-galactose-induced aging *in vivo* and *in vitro*. *J Ethnopharmacol* **2023**, 311, 116286.
42. Liu, J.; Meng, J.; Li, R.; Jiang, H.; Fu, L.; Xu, T.; Zhu, G.Y.; Zhang, W.; Gao, J.; Jiang, Z.H.; et al. Integrated network pharmacology analysis, molecular docking, LC-MS analysis and bioassays revealed the potential active ingredients and underlying mechanism of Scutellariae radix for COVID-19. *Front Plant Sci* **2022**, 13, 988655.
43. Dinda, B.; Dinda, M.; Dinda, S.; De, U.C. An overview of anti-SARS-CoV-2 and anti-inflammatory potential of baicalein and its metabolite baicalin: Insights into molecular mechanisms. *Eur J Med Chem* **2023**, 115629.
44. Gao, Y.; Snyder, S.A.; Smith, J.N.; Chen, Y.C. Anticancer properties of baicalein: a review. Med Chem Res 2016, 25, 1515-1523.
45. Yang, J.Y.; Ma, Y.X.; Liu, Y.; Peng, X.J.; Chen, X.Z. A Comprehensive Review of Natural Flavonoids with Anti-SARS-CoV-2 *Activity*. *Molecules* **2023**, 28, 2735
46. Lin, C.; Tsai, F.J.; Hsu, Y.M.; Ho, T.J.; Wang, G.K.; Chiu, Y.J.; Ha, H.A.; Yang, J.S. Study of Baicalin toward COVID-19 Treatment: In silico Target Analysis and *in vitro* Inhibitory Effects on SARS-CoV-2 Proteases. *Biomed Hub* **2021**, 6, 122-137.
47. Zandi, K.; Musall, K.; Oo, A.; Cao, D.; Liang, B.; Hassandarvish, P.; Lan, S.; Slack, R.L.; Kirby, K.A.; Bassit, L.; et al. Baicalein and Baicalin Inhibit SARS-CoV-2 RNA-Dependent-RNA Polymerase. *Microorganisms* **2021**, 9. 893.
48. Su, H.X.; Yao, S.; Zhao, W.F.; Li, M.J.; Liu, J.; Shang, W.J.; Xie, H.; Ke, C.Q.; Hu, H.C.; Gao, M.N.; et al. Anti-SARS-CoV-2 activities *in vitro* of Shuanghuanglian preparations and bioactive ingredients. *Acta Pharmacol Sin* **2020**, 41, 1167-1177.
49. Zhu, D.; Su, H.; Ke, C.; Tang, C.; Witt, M.; Quinn, R.J.; Xu, Y.; Liu, J.; Ye, Y. Efficient discovery of potential inhibitors for SARS-CoV-2 3C-like protease from herbal extracts using a native MS-based affinity-selection method. *J Pharm Biomed Anal* **2022**, 209, 114538.
50. Zhou, J.; Huang, J. Current findings regarding natural components with potential anti-2019-nCoV activity. *Front Cell Dev Biol* **2020**, 8, 589.
51. Song, J.B.; Zhao, L.Q.; Wen, H.P.; Li, Y.P. Herbal combinations against COVID-19: A network pharmacology, molecular docking and dynamics study. *J Integr Med* **2023**, 21, 593-604
52. Shakhsi-Niaei, M.; Soureshjani, E.H.; Babaheydari, A.K. In silico comparison of separate or combinatorial effects of potential inhibitors of the SARS-CoV-2 binding site of ACE2. *Iran J Public Health* **2021**, 50, 1028.
53. KalantarMotamedi, Y.; Eastman, R.T.; Guha, R.; Bender, A. A systematic and prospectively validated approach for identifying synergistic drug combinations against malaria. *Malar J.* **2018**, 17, 160.
54. Ianevski, A.; Giri, A.K.; Gautam, P.; Kononov, A.; Potdar, S.; Saarela, J.; Wennerberg, K.; Aittokallio, T. Prediction of drug combination effects with a minimal set of experiments. *Nat Mach Intell* **2019**, 1, 568-577.
55. Ianevski, A.; He, L.; Aittokallio, T.; Tang, J. SynergyFinder: a web application for analyzing drug combination dose–response matrix data. *Bioinformatics* **2017**, 33, 2413-2415.
56. Yadav, B.; Wennerberg, K.; Aittokallio, T.; Tang, J. Searching for drug synergy in complex dose–response landscapes using an interaction potency model. *Comput Struct Biotechnol J* **2015**, 13, 504-513.
57. Ianevski, A.; Giri, A.K.; Aittokallio, T. SynergyFinder 2.0: visual analytics of multi-drug combination synergies. *Nucleic Acids Res* **2020**, 48, W488-W493.